Nonlinear response of a photorefractive crystal in a variable field to a moving interference pattern

A. V. Dugin, B. Ya. Zel'dovich, P. N. Il'inykh, and O. P. Nesterkin

Chelyabinsk State Technical University
(Submitted 21 April 1992)
Zh. Eksp. Teor. Fiz. **102**, 1469–1483 (November 1992)

We study the mechanism of recording a static hologram by a moving interference pattern in a photorefractive crystal in an external ac field. The field's frequency is equal to, or is an integral multiple of, the modulation frequency of one of the interacting beams and considerably exceeds the inverse recording time. The cases of phase and amplitude modulation are studied. The theoretical analysis is based on material equations describing the spatial separation of charge in the photorefractive crystal. The crystal used in the experiment was $Bi_{12}TiO_{20}$.

INTRODUCTION

The past decade has seen a keen interest in the nonlinear-optics photorefractive effect. The reason is the outstanding potential of photorefractive crystals (PRC) for optical processing and storage of data, transformation of wave fronts, and holographic interferometry, to name some fields of application.[1] The process of recording a holographic grating in a PRC constitutes spatial separation of charge as a result of electron photoexcitation to the conduction band with subsequent formation of a space-charge field grating. The refractive-index grating results from the Pockels effect.

The simplest mechanism of separating the space charge is the diffusion and drift of electrons in the internal photovoltaic field.[1] In crystals with fairly low electrooptic coefficients (selenites and semiconductors) the diffusion mechanism does not produce a strong refractive-index grating. By applying a constant external field the photorefractive response of the crystal can be amplified.[2] The drawback of this method is that it requires uniform illumination to exclude electrostatic screening of the field in the brightly illuminated regions. The method of recording in a rapidly varying field[3] (i.e., rapid in comparison to the time of dielectric relaxation) is free from this drawback but can be used only if the electron drift length $l_0 = E_0\mu\tau$ exceeds the period $\Lambda/2\pi = q^{-1}$ of the interference pattern being registered. Here E_0 is the amplitude of the external field applied to the crystal, and $\mu\tau$ the product of electron mobility and the time the electron spends in the conduction band (the trap lifetime in the conduction band).

A method for recording holograms in an external ac field applicable to crystals with an arbitrary drift length was suggested and verified experimentally in Refs. 4–8. It permits recording a static grating with two beams of different frequencies (a moving interference pattern) if the frequency shift between the beams coincides with the frequency of the applied field and considerably exceeds the inverse recording time. The method became known as the mechanism of synchronous detection of a moving interference pattern by an external ac field.

This paper studies the possibility of hologram recording when the modulation frequency of one of the interacting beams is equal to, or is an integral multiple of, the frequency Ω of the applied field. In this case the field of the periodically modulated wave can be represented by a Fourier series:

$$E_p(t)=E_p\exp(-i\omega t)\sum_{n=-\infty}^{\infty}a_n\exp(-in\Omega t), \tag{1}$$

where ω is the frequency of the unmodulated wave, and the a_n are the Fourier coefficients. In the case of sawtooth modulation of the phase with an infinitely steep trailing edge and a 2π amplitude there is only one nonzero term in the sum on the right-hand side of (1). We call this modulation monochromatic. But if there are several nonzero terms in (1), we call the modulation polychromatic. Below we discuss the recording of a grating in a PRC by a uniformly moving interference pattern under monochromatic modulation, and several special cases of polychromatic modulation.

MONOCHROMATIC MODULATION

Let us consider the case of monochromatic modulation of the primary wave, where the difference in frequencies of the interacting waves, $\delta\omega = \omega_p - \omega_s$, is an integral multiple of the frequency of the field applied to the crystal. Our theoretical analysis is based on the equation for the amplitude of the space-charge field,[9]

$$dE/dt+\Gamma(t)E=-mF(t), \tag{2}$$

where

$$\Gamma(t)=\frac{1+E_D/E_q-iE_0\cos\Omega t/E_q}{\tau_M(1+E_D/E_\mu-iE_0\cos\Omega t/E_\mu)}, \tag{3}$$

$$F(t)=\frac{e^{-n\Omega t}(E_0\cos\Omega t+iE_D)}{\tau_M(1+E_D/E_\mu-iE_0\cos\Omega t/E_\mu)}. \tag{4}$$

The holographic grating is recorded by the moving interference pattern

$$I=I_0+I_0\{(m/2)\exp[i(\mathbf{qr}-n\Omega t)]+\text{c.c.}\}$$

with a contrast m and an average light intensity I_0. In Eqs. (3) and (4), $E_0\cos\Omega t$ is the external field applied to the crystal; $E_D = qk_BT/e$ is the diffusion field, with k_BT the temperature in energy units and e the elementary charge; $E_q = eN_A/\varepsilon\varepsilon_0 q$ the saturation field of traps with a number density N_A; ε and ε_0 the dc dielectric constants of the PRC and vacuum, respectively; and $E_\mu = (q\mu\tau)^{-1}$ the drift field (by its physical meaning, the electron drift length exceeds $\Lambda/2\pi$ when $E_0 > E_\mu$).

 0038-5646/92/110796-08$05.00

If the difference in frequencies of the signal and primary beams, $\delta\omega$, considerably exceeds the inverse hologram-recording time τ_{sc}^{-1}, which time is primarily determined by the Maxwellian relaxation time $\tau_M = \varepsilon\varepsilon_0/\sigma$, with σ the photoconductivity induced by the light, we can average over the field's period $2\pi/\Omega$, ignoring the rapidly oscillating part of E, which is of the order of $(\Omega\tau_{sc})^{-1}$. As a result Eq. (2) assumes the form

$$dE/dt+\langle\Gamma\rangle E=-m\langle F\rangle, \tag{5}$$

where E is the slowly varying amplitude of the space-charge field grating, and $\langle\Gamma\rangle$ and $\langle F\rangle$ are the averages of the $\Gamma(t)$ and $F(t)$ functions.

Thus, for the static amplitude $E_{\sin}^{(n)} = -m\langle F\rangle/\langle\Gamma\rangle$ of the hologram we have

$$E_{\sin}^{(n)}=i^{n+1}m\frac{E_\mu E_q}{E_0^n}\frac{\{[(E_\mu+E_D)^2+E_0^2]^{1/2}-E_\mu-E_D\}^n}{[(E_\mu+E_D)^2+E_0^2]^{1/2}-E_\mu+E_q}, \tag{6}$$

where we have assumed that n is positive ($n>0$); for negative n we must replace n with $|n|$ in Eq. (6). The subscript sin indicates the shape of the field on the crystal.

A solution for recording a static interference pattern was found in Ref. 3 and has the form

$$E_{\sin}^{(0)}=-imE_q\frac{[(E_\mu+E_D)^2+E_0^2]^{1/2}-E_\mu}{[(E_\mu+E_D)^2+E_0^2]^{1/2}-E_\mu+E_q}. \tag{7}$$

As is known, the effectiveness of nonstationary mechanisms of hologram recording greatly depends on the relation between the electron drift length and the grating period: $ql_0 = E_0/E_\mu$ (Refs. 3 and 8). Hence, in further discussions of the recording process we ignore electron diffusion and trap saturation:

$$E_D=E_q^{-1}=0. \tag{8}$$

As for the applied external field, its amplitude is assumed constant and is limited by the field of surface breakdown of the crystal. Hence, $l_0 = \mu\tau E_{0,\max}$ is a parameter indicative of a specific crystal sample.

Thus, if conditions (8) are met, we have the following limiting cases for $E_{\sin}$:

$$E_{\sin}^{(n)}=\begin{cases}\dfrac{i^{n+1}m}{2^n}\left(\dfrac{E_0}{E_\mu}\right)^{n-1}E_0, & Q\ll 1, \quad (9a)\\ i^{n+1}mE_\mu, & Q\gg 1, \quad (9b)\end{cases}$$

$$E_{\sin}^{(0)}=\begin{cases}-\dfrac{im}{2}\left(\dfrac{E_0}{E_\mu}\right)E_0, & Q\ll 1, \quad (10a)\\ -imE_0, & Q\gg 1. \quad (10b)\end{cases}$$

The maximum amplitude of the space-charge field $E_{\sin}^{(n)}$ with conditions (8) met is attained at $Q = (n^2-1)^{1/2}$ ($n>1$):

$$E_{\max}^{(n)}=i^{n+1}mE_0\left[\frac{(n-1)^{n-1}}{(n+1)^{n+1}}\right]^{1/2}. \tag{11}$$

When a static interference pattern ($n=0$) is recorded, the maximum amplitude of the space-charge field $E_{\sin}^{(0)}$ asymptotically tends to $-imE_0$ for large spatial grating frequencies q. In the case of $n=1$, $E_{\sin}^{(1)}$ attains its maximum value $-mE_0/2$ for small values of q.

Let us summarize the results of our theoretical analysis. The amplitude of the space-charge field, $E_{\sin}^{(n)}$, realized in the recording the hologram by the signal and primary beams with a frequency difference $n\Omega$ in an external ac field $E_0\cos\Omega t$ increases in proportion to q^{n-1} ($n>1$) for small $q<l_0^{-1}$ and decreases like q^{-1} for large $q>l_0^{-1}$. Examining the dependence of the grating amplitude on the amplitude of the external field, we note that the grating amplitude is proportional to E_0^n for small $Q<1$ and tends to E_μ for $Q>1$. The maximum value $E_{\max}^{(n)}$ asymptotically decreases in proportion to n (for large values of n). We also note that a sizable photorefractive response of the crystal to waves with a frequency difference $n\Omega$ ($n\neq 1$) is realized only in crystals with large drift lengths, that is, when the condition $Q = ql_0 = E_0/E_\mu > 1$ is met. As for the lock-in detection method ($n=1$), hologram recording is possible in crystals with large drift lengths and with small drift lengths, being more effective in the latter. The hologram amplitude $E_{\sin}^{(1)}$ depends on q like $E_{\sin}^{(1)}\sim E^\mu\sim q^{-1}$, starting at $mE_0/2$ for small $q<l_0^{-1}$.

Figure 1 depicts the amplitude of the space-charge field, $E_{\sin}^{(n)}$, as a function of the spatial grating frequency q with conditions (8) met and $\mu\tau = 2.3\times10^{-8}$ cm^2 V^{-1}, which coincides in order of magnitude with the data from the literature on the $Bi_{12}TiO_{20}$ crystal.[1,10] It must be noted that Eqs. (9)–(11) are valid only if there is no trapping-center saturation and no electron diffusion. Allowing for trap saturation leads to a decrease in the hologram amplitude for large values of q, and allowing for electron diffusion also leads to a decrease in the amplitude of the space-charge field for large q (Refs. 4–6).

Figures 2(a) and (b) depict the qualitative spectrum of the photorefractive response of the crystal when hologram recording is done in a sinusoidal field, for two different values of parameter Q. A small frequency detuning $\Delta\Omega(\delta\omega = n\Omega + \Delta\Omega)$ results in the holographic grating moving with a velocity of $\Delta\Omega/q$ and a decrease in its amplitude:

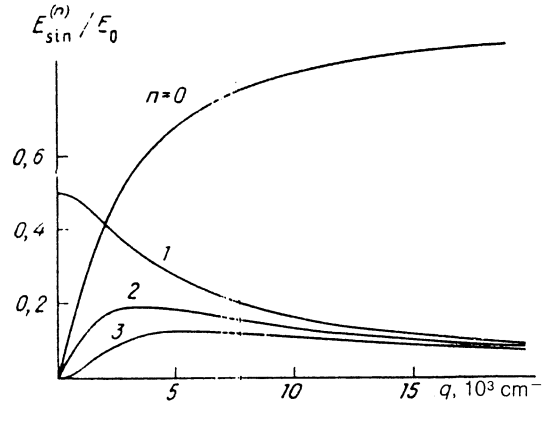

FIG. 1. Theoretical curves representing the amplitude of the space-charge field, $E_{\sin}^{(n)}$ (in units of E_0), as a function of the spatial grating frequency q in the case of a sinusoidal field $E_0\cos\Omega t$ acting on the crystal, with $E_D = E_q^{-1} = 0$ and $E_\mu = (\mu\tau q)^{-1} = (2.3\times10^{-8}q)^{-1}$.

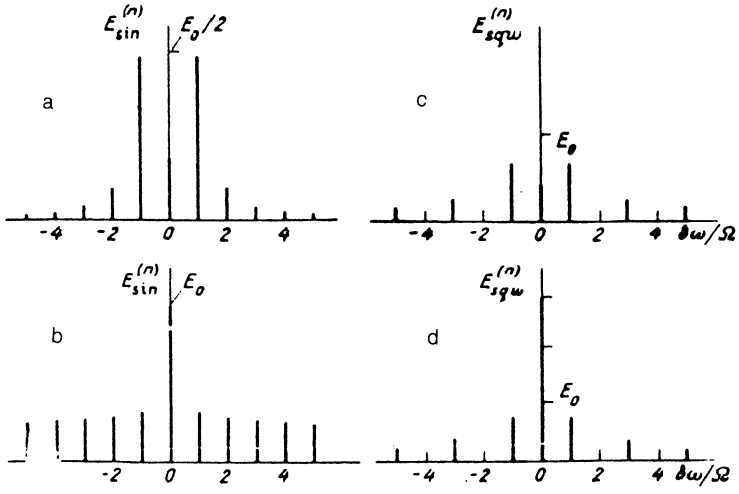

FIG. 2. The spectrum of the photorefractive response of a crystal to a moving interference pattern ($\delta\omega$ is the frequency difference of the interacting beams): (a) and (b), in a sinusoidal field $E_0 \cos\Omega t$; and (c) and (d), in a sign-alternating meander-type field $E_0 \operatorname{sgn}(\cos \Omega t)$. Cases (a) and (c) correspond to $E_0/E_\mu = 0.3$, and (b) and (d) to $E_0/E_\mu = 3$.

$$E_{\sin}^{(n)}(\Delta\Omega) = \frac{E_{\sin}^{(n)}(0)}{1 - i\Delta\Omega\tau_{sc}} \exp(-i\Delta\Omega t). \tag{12}$$

Thus, the spectral lines in Fig. 2 are Lorentzian with the width determined by the inverse hologram relaxation time, $\tau_{sc}^{-1} = \langle\Gamma\rangle$ (Ref. 5).

If the recording of the holographic grating is done in a sign-alternating meander-type field $E_0 \operatorname{sign}(\cos \Omega t)$, the respective solution to Eq. (5) has the form

$$E_{sqw}^{(n)} = \begin{cases} -imE_q \dfrac{E_0^2 + E_D(E_D+E_\mu)}{E_0^2 + (E_D+E_q)(E_D+E_\mu)} & n=0, \quad (13a) \\ \dfrac{[(-1)^n - 1]mE_0}{\pi n} \dfrac{E_\mu E_q}{E_0^2 + (E_D+E_q)(E_D+E_\mu)}, & n \geqslant 1. \quad (13b) \end{cases}$$

When conditions (8) are met, these formulas become simpler:

$$E_{sqw}^{(n)} = \begin{cases} -im\left(\dfrac{E_0}{E_\mu}\right)E_0, & n=0, \quad (14a) \\ \dfrac{[(-1)^n - 1]mE_0}{\pi n}, & n \geqslant 1. \quad (14b) \end{cases}$$

Note that in a meander field the holographic grating is not recorded in the case of even harmonics, that is, when the difference in frequencies of the primary and signal beams is $2\Omega, 4\Omega, \ldots (n = 2,4,\ldots)$. Also, the amplitude of a hologram recorded in a meander field depends neither on the spatial frequency q nor on the parameter Q for $n \neq 0$. In contrast to recording in a sinusoidal field for $Q \ll 1$, there is no proportionality to E_0^n, since a meander field contains all odd harmonics, whose contribution is described by the factor $1/n$ in Eq. (14b). Accordingly, for $Q \gg 1$ the grating amplitude is not restricted to E_μ. Hence, hologram recording in a meander field is preferable to recording in a sinusoidal, where large values of Q (large values of the electron drift length) are required.

Qualitative spectra of the photorefractive response of a crystal in a meander field are depicted in Figs. 2(a) and (d).

The phases of the gratings recorded by different harmonics merit a separate discussion. In the recording in a sinusoidal field the odd harmonics have an alternating phase factor ± 1, while in a meander field all these harmonics are in antiphase with the interference pattern (we are speaking of their position at the zero moment in time, when the field attains its maximum value). The even harmonics, however, in a sinusoidal field possess a factor $\pm i$, and in a meander field they are not recorded.

Experimental investigations were conducted with two samples of a $Bi_{12}TiO_{20}$ crystal: the one with a large electron drift length in comparison to the holographic grating period (for $\Lambda < 10\ \mu$m), BTO1, and the one with a small electron drift length, BTO2. The assumptions about the electron drift length were made on the basis of a degenerate two-wave interaction in the ac field.[3]

Figure 3 depicts the experimental setup for studying the nondegenerate two-wave interaction in PRC. A 1-mW helium-neon laser ($\lambda = 0.63\ \mu$m) was used as a source of coherent radiation. A beam-splitting plate *5* was employed to form the two beams recording the holographic grating in the crystal. The beam reflected by plate *5* was used as the signal beam $E_s \exp(-i\omega t)$. The primary beam passed through plate *5* and was reflected by mirror *4* mounted on a piezoelectric ceramic cylinder. The movements of mirror *4* were due to a sawtooth voltage applied to the cylinder. The voltage across the cylinder increased linearly to its maximum value, which resulted in a 2π phase shift in the primary beam, and then dropped rapidly to zero (the trailing-edge to leading-edge ratio did not exceed 0.01). The frequency of the primary beam reflected by mirror *4* was shifted by a quantity $n\Omega (n = 1,2,3,4)$, an integral multiple of the frequency of the field on the crystal. This was done by a specially manufactured frequency multiplier driving the generator of sawtooth pulses fed to the piezomirror. The frequency shift in the primary beam was monitored by an auxiliary interferometer consisting of elements *1–4* and a photodetector (PD). In front of the photodetector was placed a diaphragm with a diameter roughly equal to the period of the interference pattern at the exit from the interferometer. The signal from the photodetector was fed to an oscilloscope on whose screen sinusoidal oscillations were observed at a frequency equal to the frequency difference of the interacting beams. The auxiliary interferometer was used only for monitoring the fre-

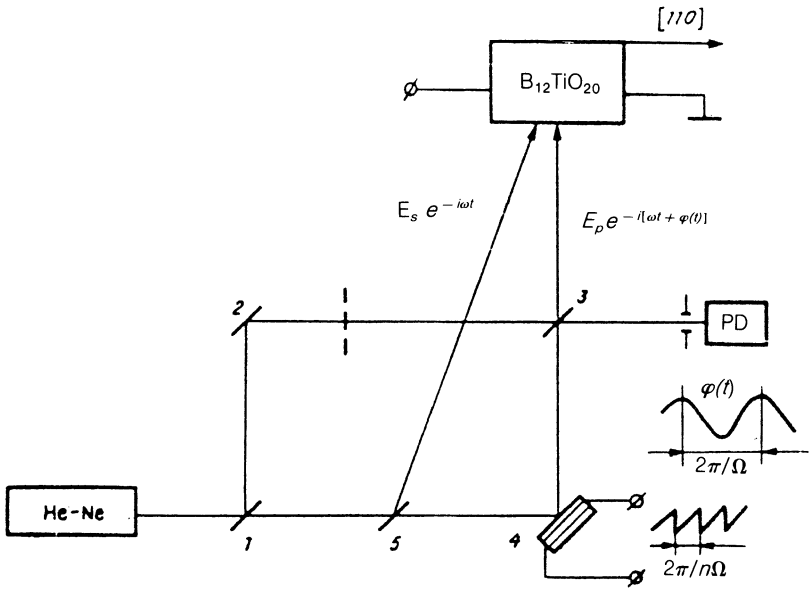

FIG. 3. The schematic of the experimental device.

quency shift in the primary wave $E_p \exp[-i(\omega+n\Omega)t]$, and the ray from mirror *2* was blocked when the waves were interacting in the crystal.

The polarizations of the interacting waves were fixed in such a manner that they would assume, owing to intrinsic optical activity, the values $\pm 45°$ in the plane of incidence in the middle of the crystal, approaching the intrinsic polarizations for the given orientation of the crystal.[1,4] The front face of the crystal was positioned at right angles to the bisector of the angle between the incident beams which formed the periodic interference pattern moving with a velocity $v = n\Omega/q$. The direction of the grating's wave vector **q** coincided with the direction of the electric field applied to the crystal along the [110] axis.

The field on the crystal had either a sinusoidal time dependence $E_0 \cos \Omega t$ ($\Omega/2\pi = 50$ Hz) or a meander-type time dependence $E_0 \sin(\cos \Omega t)$ ($\Omega/2\pi = 60$ Hz). The grating period $\Lambda = \lambda/\sin(\theta/2)$, with θ the angle between the signal and primary waves and λ the wavelength of the incident light, was varied by moving the beam-splitting plate *5*, with the path difference of the recording beams always remaining smaller than the laser's coherence length. The diffraction efficiency was determined when the hologram was read by the primary beam with the signal beam blocked.

The choice of the intensity ratio of the signal and primary beams merits separate consideration. The thing is that as a result of diffraction two new waves, $E_s' \exp(-i\omega t)$ and $E_p' \exp[-i(\omega+n\Omega)t]$, appear on the static hologram of the initial waves $E_s \exp(-i\omega t)$ and $E_p \times \exp[-i(\omega+n\Omega)t]$. The pairs of equal-frequency waves, $E_s - E_s'$ and $E_p - E_p'$, record two secondary gratings owing to electron diffusion or drift in the external ac field.[4,6] It can easily be shown that these secondary self-diffraction gratings are in antiphase with each other. Thus, if the amplitudes are equal, the effect of self-diffusion gratings, which distorts the functional dependence of the amplitude of a recorded hologram on the spatial frequency, is nil. Hence, although the theoretical analysis was done for the case of a low-contrast interference pattern, $m \ll 1$, the experimental results were obtained for $m = 1$ and, as the reasoning below shows, confirm the basic conclusions of the theory.

Figure 4 depicts the experimental data obtained with the BTO 1 crystal (large diffusion lengths) for the first harmonics of the phase modulation of the primary beam ($n = 1$). As expected, the values of the diffraction efficiency for orthogonal intrinsic polarizations coincide. This coorroborates the fact that at $m = 1$ the interference patterns of the self-diffusion grating balance each other. For a meander field on the crystal the diffraction efficiency of the recorded hologram is higher than that for a sinusoidal. The solid curves in Fig. 4 represent the theoretical dependence obtained at $N_A = 10^{15}$ cm^{-3} and $\mu\tau = 2.3\times10^{-8}$ cm^2 V^{-1}, and these are in reasonable agreement with the data from the literature on the $Bi_{12}TiO_{20}$ crystal.[1,10] The discrepancy between the experimental data and the theoretical curves for small spatial frequencies q can be explained by the transition to the Raman–Nath diffraction, provided that $q < q_B = (n_0/L\lambda)^{1/2} \approx 2\times10^3$ cm^{-1}, where n_0 is the unperturbed refractive index, and L the hologram thickness.

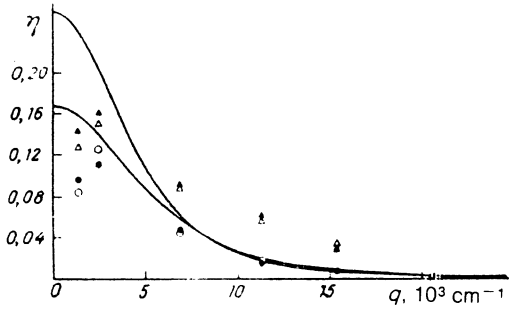

FIG. 4. The diffraction efficiency η as a function of the spatial grating frequency q ($\delta\omega = \Omega$ and $n = 1$): ○, a sinusoidal field on the crystal ($E_0 = 8$ kV cm^{-1} and $\Omega/2\pi = 50$ Hz); △, a meander field on the crystal ($E_0 = 8$ kV cm^{-1} and $\Omega/2\pi = 60$ Hz). The polarizations of the interacting waves: 45° to the plane of incidence (▲,●); −45° to the plane of incidence (△,○). The intensity ratio I_s/I_p is equal to unity. The solid curves represent the theoretical results at $\mu\tau = 2.3\times10^{-8}$ cm^2 V^{-1} and $N_A = 10^{15}$ cm^{-3}.

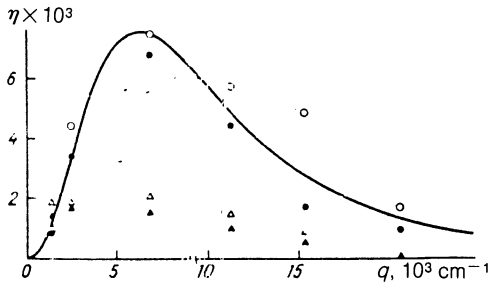

FIG. 5. The diffraction efficiency η as a function of the spatial grating frequency q ($\delta\omega = 2\Omega$ and $n = 2$). The notation is the same as in Fig. 4.

Figure 5 depicts the diffraction efficiency η as a function of the spatial grating frequency q for the case where the frequency difference of the recording beams exceeds the frequency of the field on the crystal by a factor of two ($n = 2$). The solid curve in Fig. 5 represents the theoretical dependence for recording in a sinusoidal field, a dependence obtained for the same parameters N_A and $\mu\tau$ as in Fig. 4. As for recording in a meander field, from the theoretical analysis of (14) it follows that the holographic grating should not be recorded for the even frequency-detuning harmonics of the interacting beams, $\delta\omega = n\Omega (n = 2,4,...)$. Nevertheless, we observed a nonzero diffraction efficiency of the grating. This can be explained, first, by the fact that the piezomirror does not operate in ideal conditions, as a result of which the primary beam has, in addition to a component with frequency $\omega + 2\Omega$, components with frequencies ω and $\omega + \Omega$ that interact with the signal beam, and, second, by the effect of the nonideal shape of the meander field on the crystal (the edges of the meander are not infinitely steep). Thus, further comparison of the experimental data does not seem possible: the observed photorefractive response of the crystal at $n = 3$ was found to be of the same order as that at $n = 2$ in the case of a meander field on the crystal.

A number of test experiments were conducted with the BTO2 sample (small electron drift lengths). When a sinusoidal field is applied to the crystal, significant hologram recording should be possible only for the first phase-modulation harmonic of the primary beam ($n = 1$). The response to other harmonics should be insignificant because the condition of large electron drift lengths is not met. Qualitatively these facts were found to be ture: the photorefractive response of the crystal was observed only when the frequency difference between the signal and primary beams, $\Omega/2\pi = 50$ Hz, coincided with the frequency of the ac field $E_0 \cos \Omega t$ on the crystal. Similarly, when a meander field was applied to the BTO2 crystal, significant hologram recording was observed only at $n = 1$. As for hologram recording for $n \neq 1$, this was found to be insignificant, and comparative analysis is impossible, for the reasons given above.

POLYCHROMATIC MODULATION

Let us study the possibility of recording a static hologram for the case of polychromatic modulation of the primary beam, that is, when the Fourier expansion (1) contains many components with frequencies ω, $\omega \pm \Omega$, $\omega \pm 2\Omega$, etc. The result of illuminating PRC with two beams, the modulated primary beam and the unmodulated signal beam, can be represented by a set of interference patterns that move with different velocities $(0, \pm \Omega/q, \pm \Omega/2q, ...)$. The contrast of each interference pattern is proportional to the respective coefficient a_n in the Fourier expansion (1) of the primary beam. In this section we consider two types of modulation of the primary beam: amplitude odulation via a chopper and sinusoidal phase modulation via a piezomirror.

Amplitude modulation. In the case of amplitude modulation of the primary beam the recording of the holographic grating is done by an interference pattern of the type

$$I^{chp} = \frac{I_0}{2}[\operatorname{sign}(\cos(\Omega t+\varphi)) + 1]\left[1 + \frac{m}{2}\exp(iqx) + \text{ cc.}\right], \tag{15}$$

where φ is the phase shift between the modulated signal and the ac field on the crystal. To find the amplitude of the recorded hologram we use Eq. (5). Averaging $\Gamma(t)$ and $F(t)$ over the period $2\pi/\Omega$, we arrive at the following expression for the amplitude of the space-charge field in the case of a sinusoidal field $E_0 \cos\Omega t$ on the crystal:

$$E_{\sin}^{chp} = -\frac{imE_0}{\pi Q}\left[\frac{\pi}{2}(1+Q^2)^{1/2} - \operatorname{tg}^{-1}\left(\frac{i(1+Q^2)^{1/2}}{Q\cos\varphi}\right)\right]. \tag{16}$$

Here the subscript designates the type of field on the crystal and the superscript the type of modulation. Depending on the relation between the electron drift length and the spatial grating period, $Q = ql_0 = E_0/E_\mu$, we have two limiting cases:

$$E_{\sin}^{chp} = \begin{cases} -\dfrac{mE_0}{\pi}\cos\varphi, & Q \ll 1. \quad (17a) \\ -imE_0/2. & Q \gg 1. \quad (17b) \end{cases}$$

Equation (17a) shows that the amplitude of the space-charge field depends on the phase shift φ only when the parameter Q is small.

For hologram recording in a sign-alternating meander field $E_0 \operatorname{sgn}(\cos \Omega t)$ the respective solution to Eq. (5) has the form

$$E_{sqw}^{chp} = \begin{cases} -\dfrac{mE_0}{2\pi}(\pi - 2\varphi + i\pi Q), & 0 < \varphi < \pi \\ -\dfrac{mE_0}{2\pi}(-3\pi + 2\varphi + i\pi Q), & \pi < \varphi < 2\pi. \end{cases} \tag{18}$$

Depending on the value of Q, we have the following expressions for the amplitude of the space-charge field:

$$E_{sqw}^{chp} = \begin{cases} -\dfrac{mE_0}{2}\left(1 - \dfrac{2\varphi}{\pi}\right), & 0 < \varphi < \pi, \quad Q \ll 1 \\ -\dfrac{mE_0}{2}\left(-3 + \dfrac{2\varphi}{\pi}\right), & \pi < \varphi < 2\pi, \quad Q \ll 1 \\ -imE_0 Q/2, & Q \gg 1. \end{cases} \quad \begin{matrix} \\ (19a) \\ (19b) \end{matrix}$$

Let us compare the effectiveness of hologram recording when an interference pattern of type (15) acts on the PRC to which a sinusoidal or meander field is applied. Formulas (17) and (19) show that recording in a meander field makes it possible to obtain a large photorefractive response of the

crystal for small and large values of Q. With large drift lengths ($Q \gg 1$) hologram recording in a meander field is Q times more effective than in a sinusoidal [Eqs. (17b) and (19b)] because the main contribution in hologram recording is provided by the unshifted component of the primary beam ($n = 0$) and, hence, by the equal-frequency mechanism of recording in an ac field [Eqs. (10b) and (14a)].

The experimental device used to verify the functional dependences resulting from the theoretical investigation of hologram recording for amplitude modulation of the primary beam is basically similar to the one depicted schematically in Fig. 3. Amplitude modulation was done by a mechanical chopper. As a result, the primary beam consisted of periodic pulses with a frequency $\Omega/2\pi = 20$ Hz ($\Omega \gg \tau_{sc}^{-1}$) and a unit duty cycle. The chopping frequency of the primary beam was synchronized with the frequency of the field on the crystal. To this end a fraction of the primary beam was sent to a photodiode and was used as the driving signal of the high-voltage generator of rectangular pulses fed to the $Bi_{12}TiO_{20}$ crystal. The phase difference φ between the modulating signal and the field on the crystal was varied from 0 to 2π.

Experimental measurements were carried out with the BTO1 crystal at two values of the grating period: $\Lambda = 60\,\mu$m for simulating the condition $Q < 1$ and $\Lambda = 3\,\mu$m for $Q > 1$. Figure 6 depicts the results of studying the diffraction efficiency η as a function of the phase difference $\varphi\beta$ between the modulating signal and the meander field on the crystal ($E_0 = 8$ V cm^{-1}). At $\Lambda = 60\,\mu$m the η vs φ dependence was found [Fig. 6(a)] to correspond to formula (19a) obtained theoretically. But at $\Lambda = 3\,\mu$m no dependence of η on φ was observed [Fig. (6b)]. The marked decrease in diffraction efficiency at $\Lambda = 3\,\mu$m can be explained by electron diffusion and trap saturation. These were not taken into account when the recording process was considered theoretically.

Phase modulation. One of the most important types of modulation often used in practice is the sinusoidal modulation of the laser beam phase. The interference pattern formed by two beams with the phase of one sinusoidally modulated has the form

$$I^{\sin} = I_0\{1 + \tfrac{1}{2}m\exp[iqx - iA\sin(\Omega t + \varphi)] + \text{c.c.}\}, \quad (20)$$

where A is the amplitude of the phase-modulation signal. It is impossible to derive a simple analytical expression for the amplitude of the recorded hologram obtained as a result of the action on the crystal of such an interference pattern by averaging Eq. (5) directly. Hence, we employ the results of monochromatic analysis. The phase factor $\exp[-iA\sin(\Omega t + \varphi)]$ on the right-hand side of Eq. (5) can be written as follows:

$$\exp[-iA\sin(\Omega t + \varphi)] = \sum_{n=-\infty}^{\infty} J_n(A)\exp[-in(\Omega t + \varphi)], \quad (21)$$

where $J_n(A)$ is an n-order Bessel function. Thus, we can write the amplitude of the holographic grating in the form

$$E^{\sin} = \sum_{n=-\infty}^{\infty} J_n(A)\exp(-in\varphi)E^{(n)}, \quad (22)$$

where $E^{(n)}$ is the response of the crystal with appropriate monochromatic modulation [see Eqs. (9), (10), and (14)].

Let us examine the case of a sinusoidal field on the crystal. For electron drift lengths that are small compared to the grating period ($Q \ll 1$), the first harmonic ($n = 1$) provides the basic contribution to the sum in (22) [see Eqs. (9a) and (10a)]. For large drift lengths ($Q \gg 1$) the unshifted component ($n = 0$) of the primary beam plays the main role in hologram recording [see Eqs. (9b) and (10b)]. Allowing for the fact that $J_n(A) = -J_{-n}(A)$ and $E^{(n)} = E^{(-n)}$, we get the following expression for the hologram amplitude:

$$E_{\sin}^{\sin} = \begin{cases} imE_0 J_1(A)\sin\varphi, & Q \ll 1, \quad (23a) \\ imE_0 J_0(A), & Q \gg 1. \quad (23b) \end{cases}$$

As in the situation with amplitude modulation [see Eqs. (17a) and (19a)], a dependence on the phase shift φ between the ac field on the crystal and the modulating signal exists only at small values of parameter Q.

For a meander field on the crystal only odd harmonics in the primary beam record the holographs grating [see Eqs. (14a) and (14b)]. As a result we arrive at the following expression for the amplitude of the space-charge field:

$$E_{sqw}^{\sin} = -iE_0\left[J_0(A)Q + \frac{4}{\pi}\sum_{l=0} J_{2l+1}(A)\frac{\sin[(2l+1)\varphi]}{2l+1}\right], \quad (24)$$

which has two limiting cases depending on the values of Q,

$$E_{sqw}^{\sin} = \begin{cases} \dfrac{-4iE_0}{\pi}\displaystyle\sum_{l=0} J_{2l+1}(A)\frac{\sin[(2l+1)\varphi]}{2l+1}, & Q \ll 1, \quad (25a) \\ -iE_0 J_0(A)Q, & Q \gg 1. \quad (25b) \end{cases}$$

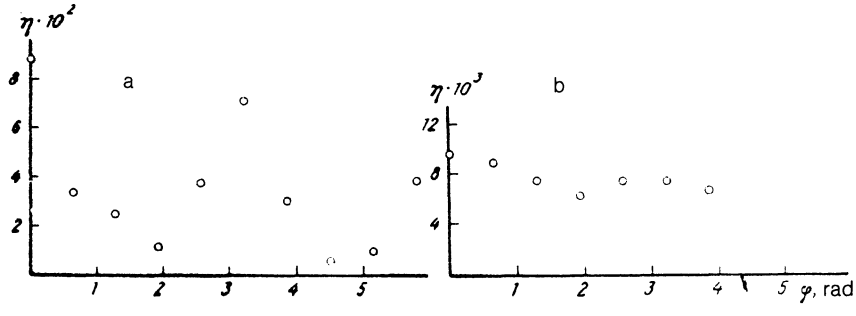

FIG. 6. The diffraction efficiency η as a function of the phase difference φ between the modulating signal and the meander field on the crystal ($E_0 = 8$ V cm^{-1}) for the case of amplitude modulation of the primary wave. The spatial grating period Λ is (a) 60 μm and (b) 3 μm.

An important aspect of this result is that for $Q \ll 1$ and $\varphi = 0$ no holographic grating is recorded.

Experimental studies of hologram recording with the primary beam phase-modulated were carried out for a sinusoidal field on the crystal. The frequency of the field was synchronized with that of the modulating signal on the piezomirror. To this end both the sinusoidal signal on the piezomirror and the ac field on the crystal were taken from the electric power line ($\Omega = 50$ Hz). The amplitude of the modulating signal on the piezomirror was varied by a linear autotransformer and the phase of the signal by a phase shifter. The sinusoidal field was fed to the crystal through a step-up transformer, and the amplitude E_0 was 8 Vcm^{-1}. What was varied in the experiments was either the phase difference between the voltage across the piezomirror and the field on the crystal at a fixed amplitude of the sinusoidal signal on the piezomirror, or the amplitude of the sinusoidal voltage across the piezomirror at a fixed phase difference.

As predicted by theory [see Eq. (23a)], a dependence of the diffraction efficiency η on the phase difference φ between the voltage across the piezomirror and the field on the crystal was observed only for large grating periods, $\Lambda = 60$ μm [$Q < 1$; Fig. 7(a)]. For small grating periods, $\Lambda = 3\,\mu$m, no φ-dependence in η was noted [Fig. 7(b)]. The discrepancy between η at $\varphi = 0$ and η at $\varphi = \pi$ in Fig. 7(a) can be explained as follows. The theoretical expressions for the amplitude of the recorded grating were obtained in two limiting cases: $Q \ll 1$ and $Q \gg 1$. The first yields (23a) for the dependence on the phase difference between the modulating signal and the field on the crystal, and the second yields (23b), which contains no such dependence. Hence, if we assume that there is a small φ-independent term α in (23a), the $\eta(\varphi) \propto (\sin\varphi + \alpha)^2$ functional dependence and the respective solid curve in Fig. 7(a) provide a good description for the experimental data.

In the studies of the dependence of the diffraction efficiency on the amplitude of the sinusoidal signal on the piezomirror (the phase-modulation amplitude A) the phase difference φ between the modulating signal and the field on the crystal was zero. To compare the obtained η vs A dependence with the theoretical expressions (23a) and (23b), which are proportional to the zeroth- and first-order Bessel functions $J_1(A)$ and $J_0(A)$, respectively, we laid off on the abscissa not the amplitude of the sinusoidal voltage across the piezomirror but the corresponding phase shift of the primary beam. The correspondence of the voltage across the piezomirror to the phase shift of the primary beam was determined in monochromatic modulation: an auxiliary interferometer (see Fig. 3) was used to monitor the interference pattern formed by the two beams, one of which (the primary) was modulated by sawtooth voltage applied to the piezomirror, with the maximum amplitude of this voltage chosen in such a way that the phase of the primary beam varied by 2π. In our case this voltage amounted to 120 V. Thus, by changing the voltage and assuming that the response of the piezomirror is linear one can vary the phase of the primary beam.

Figure 8 depicts the dependence of the diffraction efficiency η on the amplitude A of the phase modulation of the primary wave. As the theoretical analysis predicted, for large values of the recorded-grating period ($\Lambda = 60\,\mu$m) the η vs A dependence is proportional to the square of the first-order Bessel function [Fig. 8(a)]; accordingly, for small values of the period ($\Lambda = 3$ μm) it is proportional to the square of the zeroth-order Bessel function [Fig. (8b)]. The insignificant discrepancy between the experimental data and the approximations by the functions $J_1^2(A)$ and $J_0^2(A)$ can be explained by the effect of other frequency components, since the limiting cases of $Q \gg 1$ and $Q \ll 1$ can be realized in practice only with finite accuracy.

CONCLUSION

In many media phase gratings can be recorded owing to the Brillouin or Raman nonlinearity.[11] The optimum phase shift between the interacting waves in such cases is determined by the medium's resonance frequency. It reaches 10^9–10^{13} Hz and is affected only slightly by external fields. In photorefractive media, the effectiveness of the studied mechanisms of recording drops considerably if the frequency difference between the recording waves exceeds the inverse of the hologram-formation time, which is determined primarily by the Maxwell relaxation time τ_M. Thus, the zero velocity of motion of the interference pattern is resonant for most photorefractive recording mechanisms. An exception is the mechanism of drift in a dc field, where the electron drift length exceeds the interference-pattern period, that is, $ql_0 > 1$. When a moving interference pattern is illuminated, the hologram moves in step with it and the holographic grating amplitude increases resonantly at a resonant velocity $v_{\mathrm{res}} = \Omega_{\mathrm{res}}/q = (q^2 l_0 \tau_M)^{-1}$ (Refs. 12 and 13). It must be noted that the resonance frequency shift $\Omega_{\mathrm{res}} = (ql_0\tau_M)^{-1}$

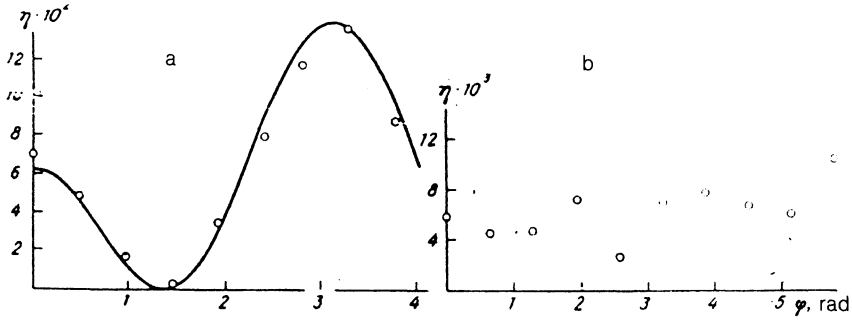

FIG. 7. The diffraction efficiency η as a function of the phase difference φ between the modulating signal and the sinusoidal field on the crystal ($E_0 = 8$ kV cm^{-1}) for the case of phase modulation of the primary wave (at a fixed modulation amplitude A). The spatial grating period Λ is (a) 60 μm and (b) 3 μm.

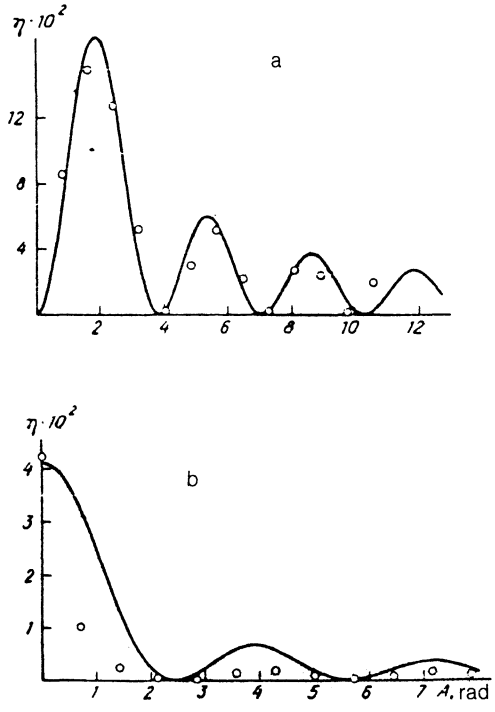

FIG. 8. The diffraction efficiency η as a function of the phase-modulation amplitude A of the primary wave (at a fixed phase difference φ). The spatial grating period Λ is (a) 60 μm and (b) 3 μm.

is smaller than the inverse Maxwell relaxation time but greater than the inverse record-erase time $\tau_{sc}^{-1} = (ql_0^{-2})\tau_M^{-1}$.

In this paper we have shown that in recording in an ac field of frequency Ω the spectrum of the photorefractive response of a crystal to an interference pattern moving with a velocity $\delta\omega/q$ ($\delta\omega \gg \tau_{sc}^{-1}$) broadens and consists of bands whose frequencies are integral multiples of the external-field frequency, $\delta\omega = n\Omega$ (see Fig. 2). As a result of our analysis we have determined the relative height of the lines. The linewidth is determined by the inverse recording time, and the position of the lines is related to the external-field frequency. As for the maximum frequency of the ac field at which synchronous detection of the moving interference pattern is stil possible, the physical measure of limiting the frequency of the detecting field is the inverse of the time that an electron stays in the conduction band, τ^{-1}. If $\Omega \gg \tau^{-1}$, the photoexcited electrons oscillate in the external field and are captured by trapping centers without a substantial space-charge redistribution owing to the averaging over the electron ensemble. Thus, the frequency of the detecting field, Ω, can vary between τ_{sc}^{-1} and τ^{-1}.

We have also studied both theoretically and experimentally the mechanism by which a static grating is recorded by a moving interference pattern in an external ac field. The effectiveness of hologram recording by this mechanism is found to depend primarily on the relation between the electron drift length and the period of the recorded grating. Both phase and amplitude modulations of one of the interacting beams have been investigated.

We are grateful to N. D. Kundikova and V. S. Liberman for fruitful discussions of the present paper.

[1] *Photorefractive Materials and Their Applications*, edited by P. Gunter and J.-P. Huignard, 2 books, Springer, Berlin (1988, 1989).
[2] A. Marrakchi and J.-P. Huignard, Opt. Commun. **39**, 249 (1981).
[3] S. I. Stepanov and M. P. Petrov, Opt. Commun. **53**, 292 (1985).
[4] B. Ya. Zel'dovich, P. N. Il'inykh, and O. P. Nesterkin, Zh. Eksp. Teor. Fiz. **98**, 861 (1990) [Sov. Phys. JETP **71**, 478 (1990)].
[5] P. N. Il'inykh, O. P. Nesterkin, and B. Ya. Zel'dovich, Opt. Lett. **16**, 414 (1991).
[6] B. Ya. Zel'dovich, P. N. Il'inykh, and O. P. Nesterkin, J. Moscow Phys. Soc. **1**, 153 (1991).
[7] P. N. Il'inykh, O. P. Nesterkin, and B. Ya. Zel'dovich, Opt. Commun. **80**, 249 (1991).
[8] B. Ya. Zel'dovich and O. P. Nesterkin, J. Moscow Phys. Soc. **1**, 231 (1991).
[9] N. V. Kuchtarev, V. B. Markov, S. G. Odoulov, M. S. Soskin, and V. L. Vinetski, Ferroelectrics **22**, 949 (1979).
[10] S. I. Stepanov, in *Optical Holography with Recording in 3D Media*, edited by Yu. N. Denisyuk, Nauka, Leningrad (1986), p. 17.
[11] B. Ya. Zel'dovich, N. F. Pilipetskiĭ, and V. V. Skunov, *Inversion of Wave Fronts*, Nauka, Moscow (1985).
[12] Ph. Refrigier, L. Solymar, H. Raibenbach, and J.-P. Huignard, J. Appl. Phys. **58**, 45 (1985).
[13] S. I. Stepanov, V. V. Kulikov, and M. P. Petrov, Opt. Commun. **44**, 19 (1982).

Translated by Eugene Yankovsky